

Extracellular domain of semaphorin 5A serves a tumor-suppressing role by activating interferon signaling pathways in lung adenocarcinoma cells

MING-ZHEN CHEN¹, LI-YU SU¹, PIN-HAO KO², MING-HSUAN HSU¹, LI-LING CHUANG^{3,4}, LI-HAN CHEN⁵, TZU-PIN LU^{6,7}, ERIC Y. CHUANG⁷⁻⁹, LU-PING CHOW¹⁰, MONG-HSUN TSAI^{7,11}, HSAO-HSUN HSU¹² and LIANG-CHUAN LAI^{1,7}

¹Graduate Institute of Physiology, College of Medicine, National Taiwan University, Taipei 100;

²Department of Traditional Chinese Medicine, Taoyuan General Hospital, Ministry of Health and Welfare, Taoyuan 330; ³School of Physical Therapy and Graduate Institute of Rehabilitation Science, College of Medicine, Chang Gung University; ⁴Department of Physical Medicine and Rehabilitation, Chang Gung Memorial Hospital, Taoyuan 333; ⁵Institute of Fisheries Science, College of Life Science; ⁶Institute of Epidemiology and Preventive Medicine; ⁷Bioinformatics and Biostatistics Core, Center of Genomic and Precision Medicine;

⁸Graduate Institute of Biomedical Electronics and Bioinformatics, National Taiwan University, Taipei 106;

⁹Graduate Institute of Biomedical Engineering, College of Biomedical Engineering, China Medical University, Taichung 404; ¹⁰Graduate Institute of Biochemistry and Molecular Biology, College of Medicine; ¹¹Institute of Biotechnology, National Taiwan University, Taipei 106; ¹²Division of Thoracic Surgery, Department of Surgery, National Taiwan University Hospital and National Taiwan University College of Medicine, Taipei 100, Taiwan, R.O.C.

Received March 31, 2021; Accepted November 22, 2021

DOI: 10.3892/ijo.2022.5311

Abstract. Semaphorin 5A (SEMA5A), which was originally identified as an axon guidance molecule in the nervous system, has been subsequently identified as a prognostic biomarker for lung cancer in nonsmoking women. SEMA5A acts as a tumor suppressor by inhibiting the proliferation and migration of lung cancer cells. However, the regulatory mechanism of SEMA5A is not clear. Therefore, the purpose of the present study was to explore the roles of different domains of SEMA5A in its tumor-suppressive effects in lung adenocarcinoma cell lines. First, it was revealed that overexpression of full length SEMA5A or its extracellular domain significantly inhibited the proliferation and migration of both A549 and H1299 cells using MTT, colony formation and gap closure

assays. Next, microarray analyses were performed to identify genes regulated by different domains of SEMA5A. Among the differentially expressed genes, the most significant function of these genes that were enriched was the 'Interferon Signaling' pathway according to Ingenuity Pathway Analysis. The activation of the 'Interferon Signaling' pathway was validated by reverse transcription-quantitative PCR and western blotting. In summary, the present study demonstrated that the extracellular domain of SEMA5A could upregulate genes in interferon signaling pathways, resulting in suppressive effects in lung adenocarcinoma cells.

Introduction

Lung cancer is the most commonly diagnosed cancer worldwide (11.6% of all cases) and is a leading cause of cancer-related mortality in both males and females due to the poor 5-year overall survival rate and high recurrence rate (1,2). Non-small cell lung cancer, including large cell carcinoma, squamous cell carcinoma and adenocarcinoma, is the major subtype (~80%) among lung cancer cases (3). Among these histological subtypes, adenocarcinoma is the most common one to be diagnosed in Taiwan (1,4,5).

In Western countries, 70-90% of lung cancer cases are attributed to cigarette smoking; however, in Taiwan, only 7% of female lung cancer cases are associated with smoking (6,7). Several previous studies have identified genes (e.g., *KRAS*, phosphoinositide-3-kinase, catalytic, α polypeptide and *EGFR*) (7-12) that are associated with lung cancer in non-smokers. Our previous studies revealed that one of

Correspondence to: Dr Hsao-Hsun Hsu, Division of Thoracic Surgery, Department of Surgery, National Taiwan University Hospital and National Taiwan University College of Medicine, 8 Chung-Shan S Road, Taipei 100, Taiwan, R.O.C.
E-mail: ntuhsu@gmail.com

Professor Liang-Chuan Lai, Graduate Institute of Physiology, College of Medicine, National Taiwan University, 1 Sec1 Ren-Ai Road, Taipei 100, Taiwan, R.O.C.
E-mail: llai@ntu.edu.tw

Key words: lung cancer, semaphorin 5A, extracellular domain, tumor suppressor

the semaphorins, semaphorin (SEMA)5A, could potentially serve as a therapeutic biomarker (13) and demonstrated that SEMA5A inhibited tumor proliferation and migration in lung adenocarcinoma (14). However, to the best of our knowledge, the mechanism by which SEMA5A serves these roles is still unknown.

Semaphorins are a large protein family, which is divided into eight classes based on structural features and the distribution among different phyla (15). The sema domain is the distinctive structural and functional element of semaphorins (16) and is present as a single copy located at the N-terminus of semaphorins. It is crucial for signaling (17). Semaphorins were first identified as axon guidance molecules in the nervous system, participating in neuron growth and helping to determine neuronal polarity (18). Several studies have revealed that semaphorins are also involved in the immune system (19,20), the cardiovascular system (21), the musculoskeletal system (22) and tumor progression (23). For example, SEMA4D has been characterized as a pro-tumorigenic factor, inducing tumor angiogenesis in head and neck cancer cells (24). *SEMA3B* has been identified as a tumor suppressor gene, which inhibits lung cancer cell proliferation and induces apoptosis (25). SEMA6A has been demonstrated to regulate lung cancer cell apoptosis through its extracellular sema domain that attenuates intracellular signaling (26). Several studies have reported that SEMA5A can inhibit cancer cell proliferation by various mechanisms, such as the inhibition of human glioma cell motility (27), the suppression of pancreatic tumor burden (28) and the maintenance of an epithelial phenotype in malignant pancreatic cancer cells (29). However, whether SEMA5A employs similar mechanisms in lung adenocarcinoma requires further investigation.

The present study explored the roles of different domains of SEMA5A in its tumor-suppressive effects in lung adenocarcinoma cell lines using several *in vitro* assays and revealed that different SEMA5A domains have different functions in regulating tumor cell proliferation.

Materials and methods

Cell culture and treatments. A549 and H1299 lung carcinoma cell lines (Bioresource Collection and Research Center, Food Industry Research and Development Institute, Hsinchu, Taiwan) were cultured in RPMI-1640 medium (Gibco; Thermo Fisher Scientific, Inc.) supplemented with 10% FBS (MilliporeSigma) and 1% penicillin-streptomycin (Gibco; Thermo Fisher Scientific, Inc.). The cell lines were incubated at 37°C in a humidified atmosphere with 5% CO₂.

Cell line authentication. Cell experiments were performed on cells that were passaged <20 times and were routinely tested for mycoplasma using a PCR Mycoplasma Detection Kit (Applied Biological Materials, Inc.) according to the manufacturer's protocol. The cell lines were authenticated by short-tandem repeat analysis (Mission Biotech Inc.).

Plasmid construction. To overexpress the various SEMA5A domains, different plasmids were constructed by the BioMed Resource Core of the 1st Core Facility Lab, National Taiwan University College of Medicine (Taipei, Taiwan). The

constructs of 5A-Full, 5A-ECD and 5A-ICD were individually inserted into a pN1 vector, which was modified from the pEGFP-N1 vector (National Taiwan University College of Medicine, Taipei, Taiwan). pN1-6xHis/5A-Full/FLAG/Kan was constructed to overexpress SEMA5A full length with a His-tag at the N-terminus and a Flag-tag at the C-terminus. pN1-18xHis/5A-ECD/Kan was constructed to overexpress the extracellular domain with a His-tag at the N-terminus. pN1-5A-ICD/18xHis/Kan was constructed to overexpress the intracellular domain with a His-tag at the C-terminus. A schematic graph of constructs of SEMA5A Full, ECD and ICD is shown in Fig. S1.

Transfection. The A549 and H1299 cells were transfected with different SEMA5A-expressing plasmids [pN1-6xHis/5A-Full/FLAG/Kan (7,225 bp; 200 ng/μl), pN1-18xHis/5A-ECD/Kan (6,919 bp; 200 ng/μl) and pN1-5A-ICD/18xHis/Kan (4,336 bp; 200 ng/μl)] and control plasmid (pN1 vector; 3,957 bp; 200 ng/μl) using jetPRIME transfection reagent (Polyplus-transfection SA) for 10 min at room temperature according to the manufacturer's protocol. The A549 and H1299 cells were seeded in a 6-cm dish (2.5x10⁵ cells/well) and incubated at 37°C for 24 h before transfection. Cells were transfected with different SEMA5A domain plasmids using jetPRIME transfection reagent (Polyplus-transfection SA). Transfection reagent was mixed with plasmids for 10 min at room temperature, and then added into 6-cm dish along with cell culture medium. Cells were then incubated at 37°C for 24 h for RNA extraction or at 37°C for 48 h for protein extraction. Cells transfected with SEMA5A full length, SEMA5A extracellular domain and SEMA5A intracellular domain were the SEMA5A full length (5A-Full), SEMA5A extracellular domain (5A-ECD) and SEMA5A intracellular domain (5A-ICD) groups, respectively.

RNA extraction and reverse transcription-quantitative PCR (RT-qPCR) analysis. Total RNA was extracted from cultured A549 and H1299 cells using NucleoZOL reagent (Machery-Nagel GmbH) according to the manufacturer's protocol. Total RNA (1 μg) was reverse transcribed using a High-Capacity cDNA Reverse Transcription Kit (Applied Biosystems; Thermo Fisher Scientific, Inc.). The temperature protocol for reverse transcription was as follows: 25°C for 10 min, 37°C for 120 min and 85°C for 5 min, followed by 4°C forever. Subsequently, 5% of each cDNA reaction was used as the template for qPCR using OmicsGreen qPCR MasterMix (OmicsBio). The primers are shown in Table I. RT-qPCR was performed using a Step One Plus Real-Time PCR System (Thermo Fisher Scientific, Inc.). The thermocycling conditions for qPCR were: 95°C for 15 min, followed by 40 cycles of 95°C for 15 sec, 60°C for 20 sec and 72°C for 20 sec. The mRNA expression levels were normalized using *GAPDH*, and relative mRNA levels were measured using the 2^{-ΔΔC_q} method (30).

Protein extraction. Before lysis, A549 and H1299 cells were washed with cold PBS (Biomax Scientific Co., Ltd.) and samples were harvested with cell scrapers. RIPA lysis buffer (MilliporeSigma) with RNase inhibitor and protease inhibitor cocktail (MilliporeSigma) was used to lyse the cells. Total protein concentrations were detected using Protein Assay Dye Reagent

primers used for reverse transcription-quantitative PCR.

Gene	Sequence (5'-3')
<i>5A-Full</i>	F: GTGCGTCTTCAACCTGAGCG R: CCTGGTCCACGGTGCCAC
<i>5A-ECD</i>	F: GTGCGTCTTCAACCTGAGCG R: CCTGGTCCACGGTGCCAC
<i>5A-ICD</i>	F: CCTGCCCCCTTAATACCAGC R: CTTCCCAGTGAGATGTGGGTTG
<i>JAK1</i>	F: TCCAAGAACCTGAGTGTGGC R: CCTGCACCGGCTTTCATAGA
<i>JAK2</i>	F: CCTTTTTAGAGGGGAAATGAGGT R: ATGGTGTCTAAAGTGGAGTAGC
<i>TYK2</i>	F: CCATCATTCGCACCATCCT R: GTTGGTCGGATCGTAGCAGT
<i>STAT1</i>	F: GGACCGCACCTTCAGTCTTT R: TCTCATTCACATCTCTCAACTCAC
<i>STAT2</i>	F: TTCTGCCGGGACATTCAGGA R: TGGCTCTCCACAGGTGTTTC
<i>IRF9</i>	F: AGCTTGAGAGGGGCATCCTA R: GGCCCTGAAAGTACCTGACC
<i>G1P2</i>	F: GTGGACAAATGCGACGAACC R: GAAGGTCAGCCAGAACAG
<i>G1P3</i>	F: AATGCGGGTAAGGATGCAGG R: CCATTCAGGATCGCAGACCA
<i>IFIT1</i>	F: CTCTGCCTATCGCCTGGATG R: AGCTTCAGGGCAAGGAGAAC
<i>IFITM1</i>	F: CATGTCGTCTGGTCCCTGTT R: GTCACAGAGCCGAATACCAGT
<i>IFITM2</i>	F: TGAGAAAACGGAACTACTGGGG R: GAGCATCTCGTAGTTGGGAGG
<i>IFITM3</i>	F: TGCTGATCTTCCAGGCCTATG R: AGCGTGTGAGGATAAAGGGC
<i>GAPDH</i>	F: AACGGGAAGCTTGTTCATCAATGGAAA R: GCATCAGCAGAGGGGGCAGAG

5A-ECD, SEMA5A extracellular domain; 5A-Full, SEMA5A full length; 5A-ICD, SEMA5A intracellular domain; F, forward; G1P, glycogenin 1 pseudogene; IFIT1, interferon induced protein with tetratricopeptide repeats 1; IRF9, interferon regulatory factor 9; JAK, Janus kinase; R, reverse; SEMA5A, semaphorin 5A; TYK2, tyrosine kinase 2.

Concentrate (Bio-Rad Laboratories, Inc.). Membrane protein extraction was conducted using a Mem-PER™ plus membrane protein extraction kit (Thermo Fisher Scientific, Inc.) according to the manufacturer's protocol. Proteins in the cell culture medium were concentrated using a Nanosep centrifugal 10K OMEGA™ filter (Pall Life Sciences) at 300 x g for 40 min at 4°C, and BSA (1 ng/ml; Sigma-Aldrich; Merck KGaA) was added externally to the cell culture medium as the spike-in control.

Western blotting. Proteins extracted from A549 and H1299 cells and culture medium were prepared as aforementioned.

Proteins (25 µg per lane) were separated by 8 or 10% SDS-PAGE and transferred to PVDF membranes (GE Healthcare). The membranes were blocked with the undiluted Lightning Blocking Buffer (Enginlife Science Co., Ltd.) for 10 min at room temperature and incubated with the following primary antibodies overnight at 4°C: SEMA5A (dilution, 1:1,000; cat. no. PAL924Hu01; Cloud-Clone Corp.), p-STAT1 (dilution, 1:1,000; cat. no. AP0109; ABclonal Biotech Co., Ltd.), STAT1 (dilution, 1:1,000; cat. no. 10144-2-AP; ProteinTech Group, Inc.), p-STAT2 (dilution, 1:1,000; cat. no. AP0284; ABclonal Biotech Co., Ltd.), STAT2 (dilution, 1:1,000; cat. no. 72604; Cell Signaling Technology, Inc.), p-JAK1 (dilution, 1:1,000; cat. no. AP0530; ABclonal Biotech Co., Ltd.), JAK1 (dilution, 1:1,000; cat. no. 3332; Cell Signaling Technology, Inc.), p-JAK2 (dilution, 1:1,000; cat. no. AP0531; ABclonal Biotech Co., Ltd.), JAK2 (dilution, 1:1,000; cat. no. 3230; Cell Signaling Technology, Inc.), IFIT1 (dilution, 1:1,000; cat. no. 14769; Cell Signaling Technology, Inc.), G1P2 (ISG15) (dilution, 1:1,000; cat. no. 2758; Cell Signaling Technology, Inc.), ACTB (dilution, 1:5,000; cat. no. 3700; Cell Signaling Technology, Inc.), caspase-3 (CASP3) (dilution, 1:1,000; cat. no. 9662; Cell Signaling Technology, Inc.), cleaved caspase-3 (dilution, 1:1,000; cat. no. 9661; Cell Signaling Technology, Inc.) and GAPDH (dilution, 1:5,000; cat. no. 10494-1-AP; ProteinTech Group, Inc.). The secondary antibodies were goat anti-rabbit IgG HRP (dilution, 1:10,000; cat. no. RA-BZ202; Croyez Bioscience Co., Ltd.) and goat anti-mouse IgG(H+L) HRP (dilution, 1:10,000; cat. no. RA-BZ102; Croyez Bioscience Co., Ltd.). After immunoblotting, the membranes were washed with Tris-buffered saline with 0.1% Tween-20 and incubated with horseradish peroxidase-conjugated goat anti-rabbit IgG (Croyez Bioscience Co., Ltd.) or goat anti-mouse IgG (Croyez Bioscience Co., Ltd.) for 1 h at room temperature. The blotted protein bands were detected using Luminata™ Forte Western HRP Substrate in an enhanced chemiluminescence system (MilliporeSigma) with the BioSpectrum Imaging System (Analytik Jena AG). The intensities of bands were analyzed using ImageJ 1.48v (National Institutes of Health).

Cell proliferation assay. A549 and H1299 cells (3,000 cells/well) transfected with plasmids containing different SEMA5A domains, including 5A-Full, 5A-ECD, 5A-ICD or empty control plasmid, were first seeded in a 6-cm dish and transfected with different SEMA5A-expressing plasmids for 24 h. Then, the transfected cells were seeded on 96-well plates at a density of 3,000 cells/well. After incubation for 12 h, cell proliferation was measured using MTT (Bionovas Biotechnology Co., Ltd.) assays at 0, 24, 48 and 72 h. A mixture of 10 µl MTT solution and 90 µl RPMI medium was added to each well and incubated for 2 h. Dimethyl sulfoxide (99.8%; Sigma-Aldrich; Merck KGaA) was used to dissolve the purple formazan. The absorbance was measured at 570 nm. The cell growth ratio was expressed as the relative absorbance compared with 0 h.

Gap closure assay. A549 and H1299 cells transfected with plasmids containing different SEMA5A domains, including 5A-Full, 5A-ECD, 5A-ICD or empty control plasmid, were first seeded in a 6-cm dish and transfected as aforementioned for 24 h. The transfected cells were seeded in the Ibidi Culture-Insert (Ibidi GmbH) at a density of

2.5×10^4 cells/reservoir, serum-starved and incubated at 37°C overnight. After incubation, the inserts were carefully removed and the cell-free gap images were captured at 0, 12 and 24 h. Cell migration was measured by comparison with the cell-free area at 0 h using a light microscope and quantified using ImageJ 1.48v software (National Institutes of Health).

Colony formation assay. A549 and H1299 cells transfected with plasmids containing different SEMA5A domains, including 5A-Full, 5A-ECD, 5A-ICD or empty control plasmid, were seeded in a 6-cm dish and transfected as aforementioned for 24 h, and then seeded in 6-well plates at a density of 300 cells/well. After incubation at 37°C for 2 weeks, cells were fixed with 500 μ l methanol-acetic acid (Sigma-Aldrich; Merck KGaA) solution (3:1) for 10 min at room temperature and stained with 0.1% crystal violet for another 10 min at room temperature. Colonies containing >50 cells were counted and quantified using ImageJ 1.48v software (National Institutes of Health).

Flow cytometry analysis of cell cycle distribution and apoptosis. To analyze cell cycle phases and cell death, A549 and H1299 cells transfected with plasmids containing different SEMA5A domains, including 5A-Full, 5A-ECD, 5A-ICD or empty control plasmid, in the medium were harvested along with the detached cultured cells. Cell lysis buffer (0.5% Triton X-100, 0.2 μ g/ml $\text{Na}_2\text{EDTA} \cdot 2\text{H}_2\text{O}$, 1% BSA in PBS) was used to lyse cells, and cells were fixed with cold 100% methanol at -20°C overnight. After washing with PBS, cells were stained with PI (Thermo Fisher Scientific, Inc.) solution (20 μ g PI/ml; 0.1 mg RNase/ml in PBS) for 10 min on ice. The suspension was analyzed on a Beckman Coulter FC500 instrument (Beckman Coulter, Inc.) using CXP Analysis Software v2.3 (Beckman Coulter, Inc.).

Illumina microarray analysis. The levels of mRNA corresponding to the different SEMA5A constructs in A549 cells were detected and analyzed as aforementioned. Total RNA was extracted from cultured cells using NucleoZOL reagent (Machery-Nagel GmbH) according to the manufacturer's protocol. Total RNA was primed with T7 Oligo(dT) and amplified using an Illumina TotalPre RNA Amplification Kit (Ambion; Thermo Fisher Scientific, Inc.). Following the first strand cDNA synthesis, DNA polymerase and RNAase H were used to simultaneously degrade the RNA and synthesize the second strand cDNA. The double-stranded cDNA then underwent a clean-up process, and *in vitro* transcription was conducted to synthesize multiple copies of biotinylated complementary RNA (cRNA). After amplification, the cRNA was hybridized to Illumina Human HT-12 v4 BeadChips (GSGX Version 1.9.0; part number, 15002873; serial number, 200769980010; Illumina, Inc.) at 58°C for 16 h. After hybridization, the BeadChip was washed and stained with streptavidin-Cy3 dye. The intensity of the bead's fluorescence was detected using a HiScan SQ instrument (Illumina, Inc.), and the results were analyzed using BeadStudio v2011.1 software (Illumina, Inc.). After scanning, the intensity data of Illumina Human HT-12 v4 BeadChips were analyzed using the software Partek v7.0 (Partek, Inc.), and background-adjusted signals were normalized by a quantile normalization algorithm. Unpaired Student's t-tests were utilized to identify

differentially expressed genes (DEGs; Tables SI and SII). The filtering criteria were set at a fold change ≥ 1.5 or ≤ 0.67 and $P < 0.05$ compared with the empty control. Principal component analysis was utilized to evaluate the similarity of the gene expression profiles. Hierarchical clustering analysis and the Genesis 1.7.7 program (31) were used to generate a visual representation of the expression profiles. Furthermore, Ingenuity Pathway Analysis (Ingenuity Systems; Qiagen, Inc.) was applied to identify gene-gene interaction networks, biological functions and canonical pathways of DEGs. The datasets generated during the current study are available in the Gene Expression Omnibus repository (<https://www.ncbi.nlm.nih.gov/geo/query/acc.cgi?acc=GSE157062>).

Statistical analysis. Statistical analyses were performed using GraphPad Prism 8 (GraphPad Software, Inc.). Data are presented as the mean \pm SD of at least three independent experiments. Statistical significance was analyzed by unpaired Student's t-test, one-way ANOVA test and Bonferroni post hoc test or two-way ANOVA test and Bonferroni post hoc test and expressed as a P-value. $P < 0.05$ was considered to indicate a statistically significant difference. Fisher's Exact test was utilized to identify canonical pathways that differentially expressed genes were involved in. The significance of pathways was determined according to Ingenuity's default threshold ($-\log(P\text{-value}) > 1.3$).

Results

5A-Full and 5A-ECD suppress the proliferation and migration of lung adenocarcinoma cells. In previous studies, SEMA5A has been identified as a biomarker, and to suppress the proliferation and migration of lung adenocarcinoma cells (13,14). The present study first examined the effects of different SEMA5A domains on the progression of lung adenocarcinoma in A549 and H1299 cells. Total RNA was extracted at 24 h after the transfection of plasmids encoding different SEMA5A constructs, including 5A-Full, 5A-ECD and 5A-ICD. After successful overexpression of these constructs as demonstrated by RT-qPCR (Fig. 1A and B), *in vitro* functional assays were performed in both A549 and H1299 cells. The results demonstrated that 5A-Full and 5A-ECD, but not 5A-ICD, significantly ($P < 0.05$) inhibited cell proliferation in MTT assays (Fig. 1C and D) and cell migration at 24 h in gap closure assays (Fig. 1E-H) compared with empty control in both A549 and H1299 cells. Additionally, the 5A-ECD construct significantly ($P < 0.05$) decreased the colony formation of A549 cells, and the two constructs significantly ($P < 0.05$) decreased the colony formation of H1299 cells (Fig. 1I-L). However, the results of flow cytometry revealed no significant difference in the effect of different SEMA5A domains on the cell cycle distribution and apoptosis, and no significant alterations of cleaved caspase-3 were observed in A549 and H1299 cells overexpressing different SEMA5A domains (Fig. S2). These results supported the proposed tumor-suppressive role of 5A-Full in lung adenocarcinoma cells and also revealed that the extracellular domain of SEMA5A contributed to the tumor-suppressive role.

Identification of genes regulated by SEMA5A domains in A549 cells by microarray analysis. To further investigate

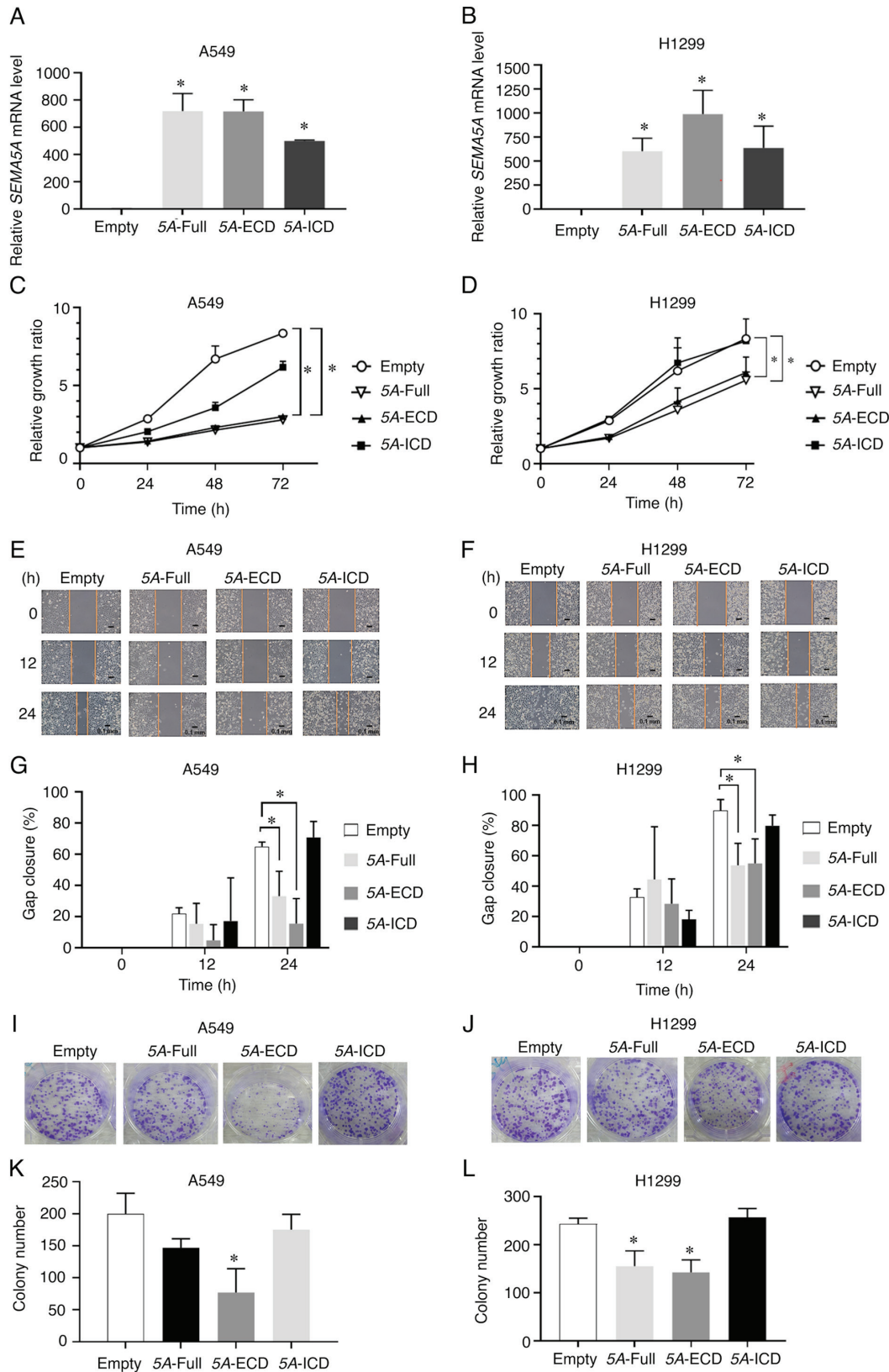


Figure 1. 5A-Full and 5A-ECD suppress the proliferation and migration of lung adenocarcinoma cells. A549 and H1299 lung adenocarcinoma cells were transfected with plasmids containing different SEMA5A domains, including 5A-Full, 5A-ECD, 5A-ICD and empty control plasmid. Relative expression levels of *SEMA5A* in (A) A549 and (B) H1299 lung adenocarcinoma cells overexpressing different SEMA5A domains examined by reverse transcription-quantitative PCR. *GAPDH* was used as the internal control. Proliferation of (C) A549 and (D) H1299 cells expressing different domains of SEMA5A assessed using MTT assays. (E and F) Gap closure assays. Representative images were captured at 0, 12 and 24 h for (E) A549 and (F) H1299 cells. Scale bar, 0.1 mm. Quantification of relative gap closure of (G) A549 and (H) H1299 cells. The percentage of wound closure was compared with the wound area at 0 h. (I and J) Colony formation assays. Representative images were captured for (I) A549 and (J) H1299 cells. (K and L) Quantification of colony counts of colony formation assays of (K) A549 and (L) H1299 cells. Experiments were repeated in triplicate, and the results are presented as the mean \pm SD. Two-way ANOVA and Bonferroni post hoc test were performed for (C and D); one-way ANOVA and Bonferroni post hoc test were performed for (A, B, G, H, K and L). * $P < 0.05$ vs. Empty. 5A-ECD, SEMA5A extracellular domain; 5A-Full, SEMA5A full length; 5A-ICD, SEMA5A intracellular domain; SEMA5A, semaphorin 5A.

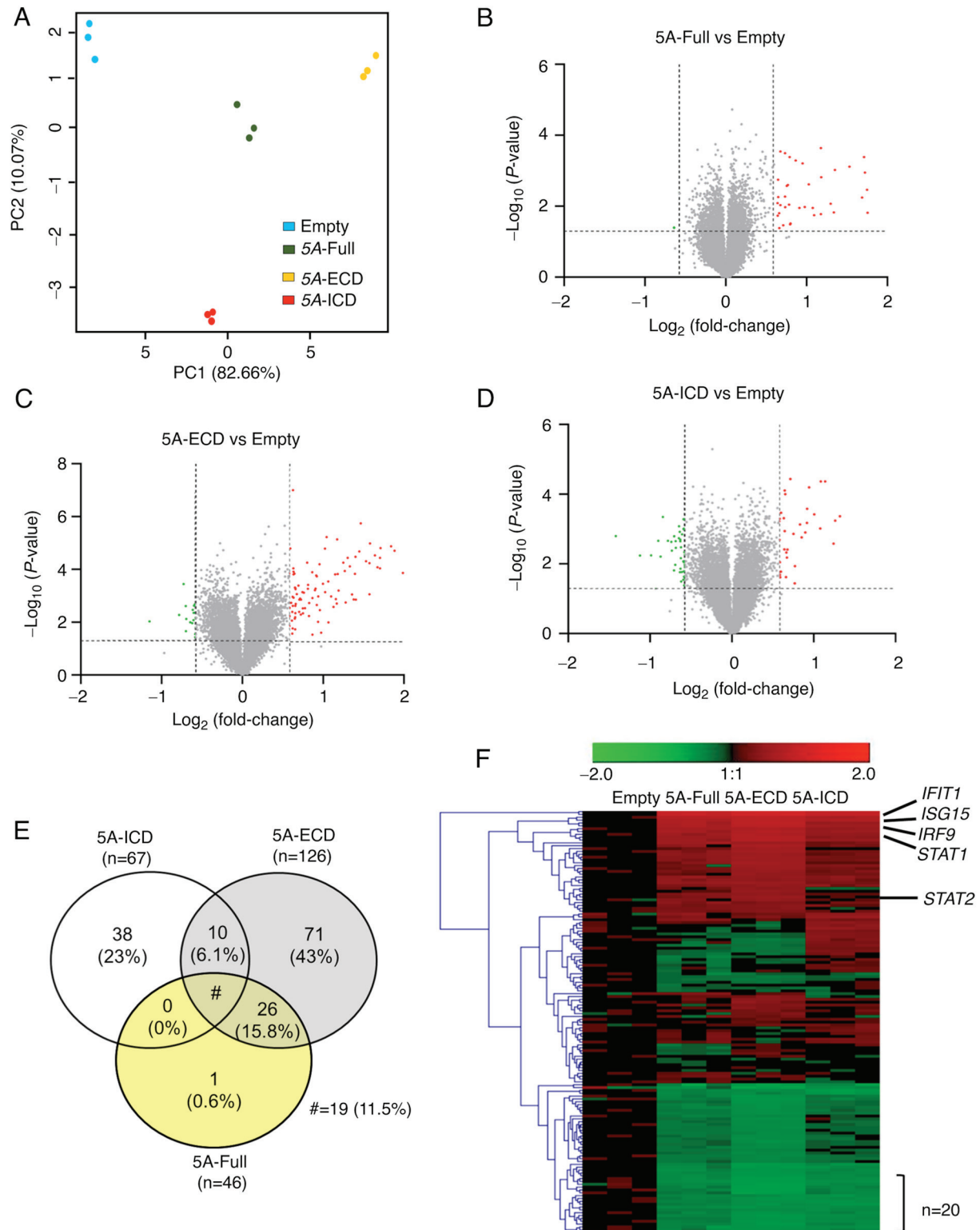


Figure 2. Identification of genes regulated by SEMA5A domains in A549 cells by microarray analysis. (A) Principal component analysis of A549 cells overexpressing different SEMA5A domains. Principal components were plotted using expression of differentially expressed probes after quantile normalization. Each dot represents one sample. (B-D) Volcano plots of DEGs in A549 cells overexpressing (B) 5A-Full, (C) 5A-ECD or (D) 5A-ICD. Dashed lines show the thresholds of fold change (≥ 1.5 or ≤ 0.67) and P-value (< 0.05). Red, upregulated genes; green, downregulated genes. (E) Venn diagram of DEGs in cells expressing different SEMA5A domains. (F) Heatmap and hierarchical cluster analysis of DEGs regulated by different SEMA5A domains. Each column represents one sample and each row represents one gene. Red, upregulated genes; green, downregulated genes. The black lines indicated representative genes involved in interferon signaling pathways. Unpaired Student's t-tests were utilized to identify DEGs. 5A-ECD, SEMA5A extracellular domain; 5A-Full, SEMA5A full length; 5A-ICD, SEMA5A intracellular domain; DEGs, differentially expressed genes; PC, principal component; SEMA5A, semaphorin 5A.

the functional roles of different SEMA5A domains, the gene expression profiles of A549 cells overexpressing different

SEMA5A domains were examined using Illumina Human HT-12 v4 BeadChips. To select the differential gene expression,

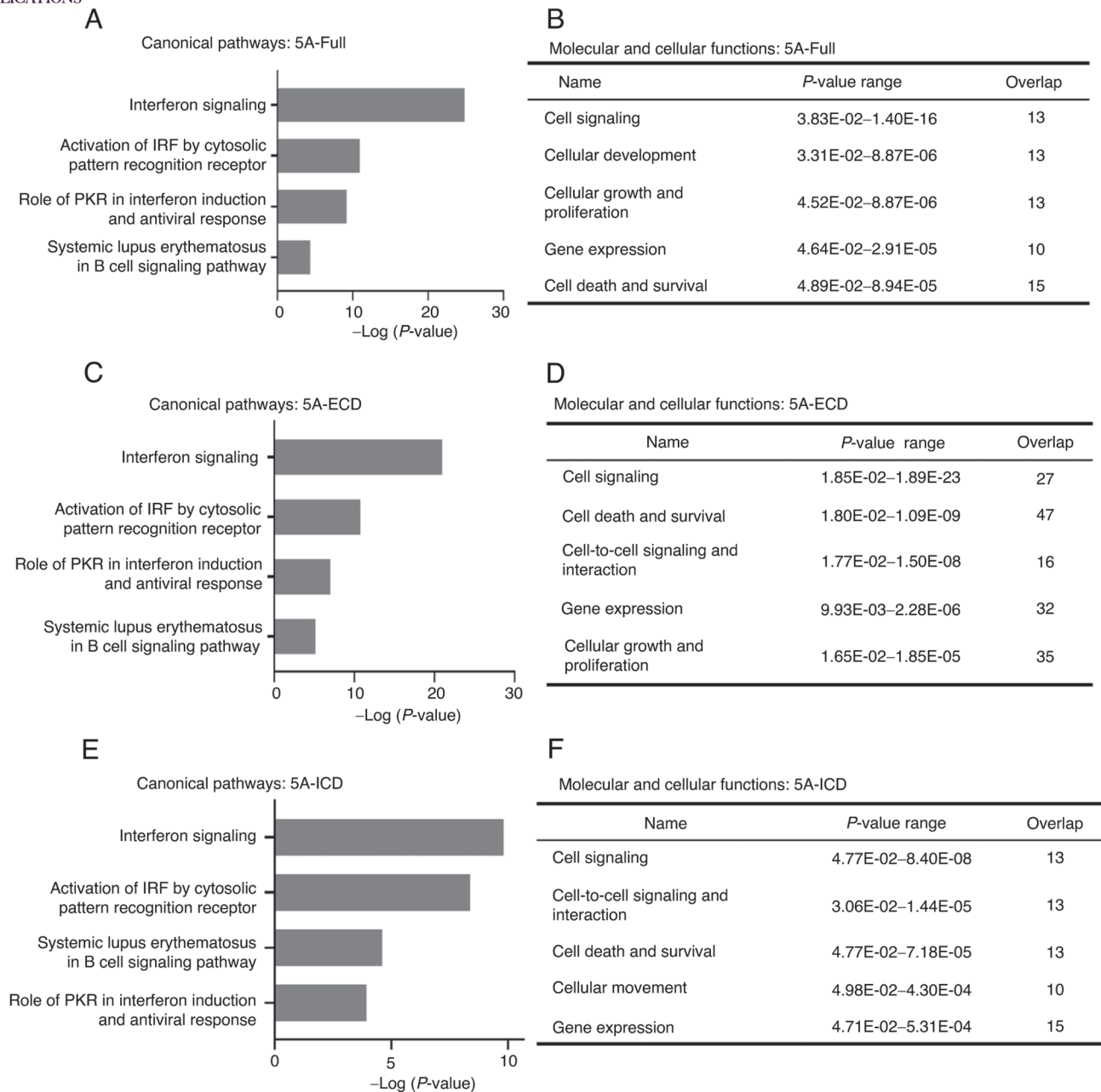


Figure 3. Ingenuity Pathway Analysis of DEGs regulated by different SEMA5A domains. (A, C and E) Top four canonical pathways of DEGs in A549 cells overexpressing (A) 5A-Full, (C) 5A-ECD or (E) 5A-ICD. The significance of pathways was determined according to Ingenuity's default threshold ($-\log(P\text{-value}) > 1.3$). Fisher's Exact test was utilized to identify canonical pathways that DEGs were enriched (B, D and F) Molecular and cellular functions of DEGs in A549 cells overexpressing (B) 5A-Full, (D) 5A-ECD or (F) 5A-ICD. 5A-ECD, SEMA5A extracellular domain; 5A-Full, SEMA5A full length; 5A-ICD, SEMA5A intracellular domain; DEGs, differentially expressed genes; IRF, interferon regulatory factor; PKR, protein kinase R; SEMA5A, semaphorin 5A.

the filtering criteria were set at a fold change ≥ 1.5 or ≤ 0.67 and $P < 0.05$ compared with the empty control. Principal component analysis was used to examine the reproducibility among samples. As shown in Fig. 2A, where each dot represents one sample, and the different colors represent different groups, the groups expressing different SEMA5A domains were separated clearly from the empty control group and from each other; however, the samples within each group were clustered together. This indicated high reproducibility within the same group and different expression profiling across groups.

A total of 165 DEGs were identified when comparing any 5A group with the empty group, including 46 DEGs in the

5A-Full group, 126 in the 5A-ECD group and 67 in the 5A-ICD group (Fig. 2B-D). Among these genes, 19 DEGs were common to all the groups expressing different SEMA5A domains, and there were 38 unique DEGs for the 5A-ICD group and 71 for the 5A-ECD group (Fig. 2E). The DEGs in the 5A-Full group were almost identical to those in the 5A-ECD group, except nucleolar protein with MIF4G domain 1 (Fig. 2E). The common gene list is shown in Table SII. All 165 DEGs were hierarchically clustered and shown in a heatmap (Fig. 2F). In general, the expression profiling of genes in the 5A-Full group was more similar to that of the 5A-ECD group than that of the 5A-ICD group.

Table II. Relative expression levels of selected differentially expressed genes in the interferon signaling pathway examined using the Illumina Human HT-12 v4 BeadChip.

Gene	Probe ID	5A-Full vs. Empty		5A-ECD vs. Empty		5A-ICD vs. Empty	
		Log ₂ (fold change)	P-value	Log ₂ (fold change)	P-value	Log ₂ (fold change)	P-value
<i>JAK1</i>	ILMN_1793384	-0.19	7.55x10 ^{-3a}	-0.16	8.61x10 ⁻²	-0.09	5.42x10 ⁻¹
<i>JAK2</i>	ILMN_1683178	0.02	4.73x10 ⁻¹	0.13	8.71x10 ^{-3a}	0.12	2.00x10 ^{-2a}
<i>TYK2</i>	ILMN_1676955	-1.13	4.80x10 ⁻¹	-0.04	4.05x10 ⁻¹	-0.29	3.46x10 ^{-3a}
<i>STAT1</i>	ILMN_1690105	1.18	1.06x10 ^{-5a}	2.52	5.48x10 ^{-6a}	0.72	2.37x10 ^{-5a}
<i>STAT2</i>	ILMN_1690921	0.77	1.08x10 ^{-4a}	1.69	1.53x10 ^{-6a}	0.29	1.89x10 ^{-4a}
<i>IRF9</i>	ILMN_1745471	1.74	1.45x10 ^{-5a}	2.38	1.85x10 ^{-5a}	1.01	2.70x10 ^{-4a}
<i>IFIT1</i>	ILMN_1699331	0.28	1.60x10 ^{-2a}	0.53	7.61x10 ^{-5a}	0.14	2.56x10 ^{-2a}
<i>IFIT1</i>	ILMN_1707695	3.39	0.00 ^a	4.71	0.00 ^a	2.93	0.00 ^a
<i>GIP2 (ISG15)</i>	ILMN_2054019	2.86	3.47x10 ^{-6a}	3.69	5.75x10 ^{-6a}	2.00	2.39x10 ^{-5a}
<i>GIP3 (IFI6)</i>	ILMN_2347798	1.74	1.02x10 ^{-3a}	3.08	1.02x10 ^{-6a}	0.95	5.47x10 ^{-6a}
<i>GIP3 (IFI6)</i>	ILMN_1687384	2.03	6.47x10 ^{-5a}	3.53	3.57x10 ^{-6a}	1.32	3.97x10 ^{-4a}
<i>IFITM1</i>	ILMN_1801246	0.79	1.28x10 ^{-5a}	1.40	2.33x10 ^{-5a}	0.32	1.22x10 ^{-3a}
<i>IFITM2</i>	ILMN_1673352	0.59	4.00x10 ^{-3a}	0.83	3.94x10 ^{-4a}	0.07	5.08x10 ⁻¹
<i>IFITM3</i>	ILMN_1805750	0.82	1.14x10 ^{-2a}	0.99	5.14x10 ^{-3a}	0.01	9.46x10 ⁻¹

^aP<0.05. 5A-ECD, SEMA5A extracellular domain; 5A-Full, SEMA5A full length; 5A-ICD, SEMA5A intracellular domain; GIP, glycogenin 1 pseudogene; IFIT1, interferon induced protein with tetratricopeptide repeats 1; IFITM, interferon induced transmembrane protein; IRF9, interferon regulatory factor 9; JAK, Janus kinase; SEMA5A, semaphorin 5A; TYK2, tyrosine kinase 2.

Next, to analyze which pathways the DEGs were involved in, Ingenuity Pathway Analysis was used to analyze the functions of DEGs in the different SEMA5A groups. The top four canonical pathways that the different SEMA5A domains were involved in were 'Interferon Signaling', 'Activation of IRF by Cytosolic Pattern Recognition Receptor', 'Systemic Lupus Erythematosus in B cell Signaling Pathway' and 'Role of PKR in Interferon Induction and Antiviral Response' (Fig. 3A, C and E). The corresponding molecular and cellular functions that different SEMA5A domains were possibly involved in included 'Cell Signaling', 'Gene Expression', 'Cellular Development', 'Cellular Movement', 'Cellular Growth and Proliferation', 'Cell-To-Cell Signaling and Interaction' and 'Cell Death and Survival' (Fig. 3B, D and F).

Expression levels of tumor suppressor genes in the interferon signaling pathway are upregulated by different SEMA5A domains. Since the DEGs were most likely involved in the interferon signaling pathway, relative expression levels of selected differentially expressed genes were compiled in Tables II and SIII. Selected genes in the interferon signaling pathways are also shown in Fig. 2F. The present study further investigated the DEGs in this pathway and validated their expression by RT-qPCR. Fig. 4A-C shows the schematic representation of the interferon signaling network from the Ingenuity Pathways Analysis canonical pathway. The DEGs in the 5A-Full group were similar to those in 5A-ECD group. In contrast to 5A-Full and 5A-ECD, overexpression of 5A-ICD did not affect STAT2 or a number of the nuclear elements of the interferon signaling pathway (e.g., *STAT1* and *IFIT3*).

To validate the expression levels of DEGs regulated by different SEMA5A domains in the interferon signaling pathway, RT-qPCR was performed to examine mRNA levels focusing on tumor suppressor genes identified in previous reports (32-39). The expression levels of interferon receptor-associated genes, such as Janus kinase 1 (*JAK1*), Janus kinase 2 (*JAK2*) and tyrosine kinase 2, were not significantly different in the various SEMA5A-expressing cells compared with the empty controls (Fig. 4D and E).

Overexpression of 5A-Full and 5A-ECD increases the amount of phosphorylated STAT1 in A549 cells. STAT1 and STAT2 have been previously identified to form heterodimers along with the DNA binding protein interferon regulatory factor 9 (IRF9) (40), and the transcription levels of these three proteins were significantly increased in A549 and H1299 cells overexpressing 5A-Full and 5A-ECD compared with the empty control cells (Fig. 4F and G). In addition, the expression levels of *STAT1* and *STAT2* were significantly different between cells expressing 5A-Full and 5A-ECD and cells expressing 5A-ICD (Fig. 4F and G).

Regarding *STAT1/2* downstream genes, the expression levels of tumor suppressor genes interferon induced protein with tetratricopeptide repeats 1 (*IFIT1*) and glycogenin 1 pseudogene (*GIP2*) in A549 and H1299 cells overexpressing 5A-Full and 5A-ECD were significantly increased compared with the empty control group (Fig. 4H and I). In A549 cells, *IFIT1* expression was significantly increased in cells overexpressing 5A-Full and 5A-ECD compared with cells overexpressing 5A-ICD (Fig. 4H). In H1299 cells, *GIP2* expression was significantly increased in cells overexpressing

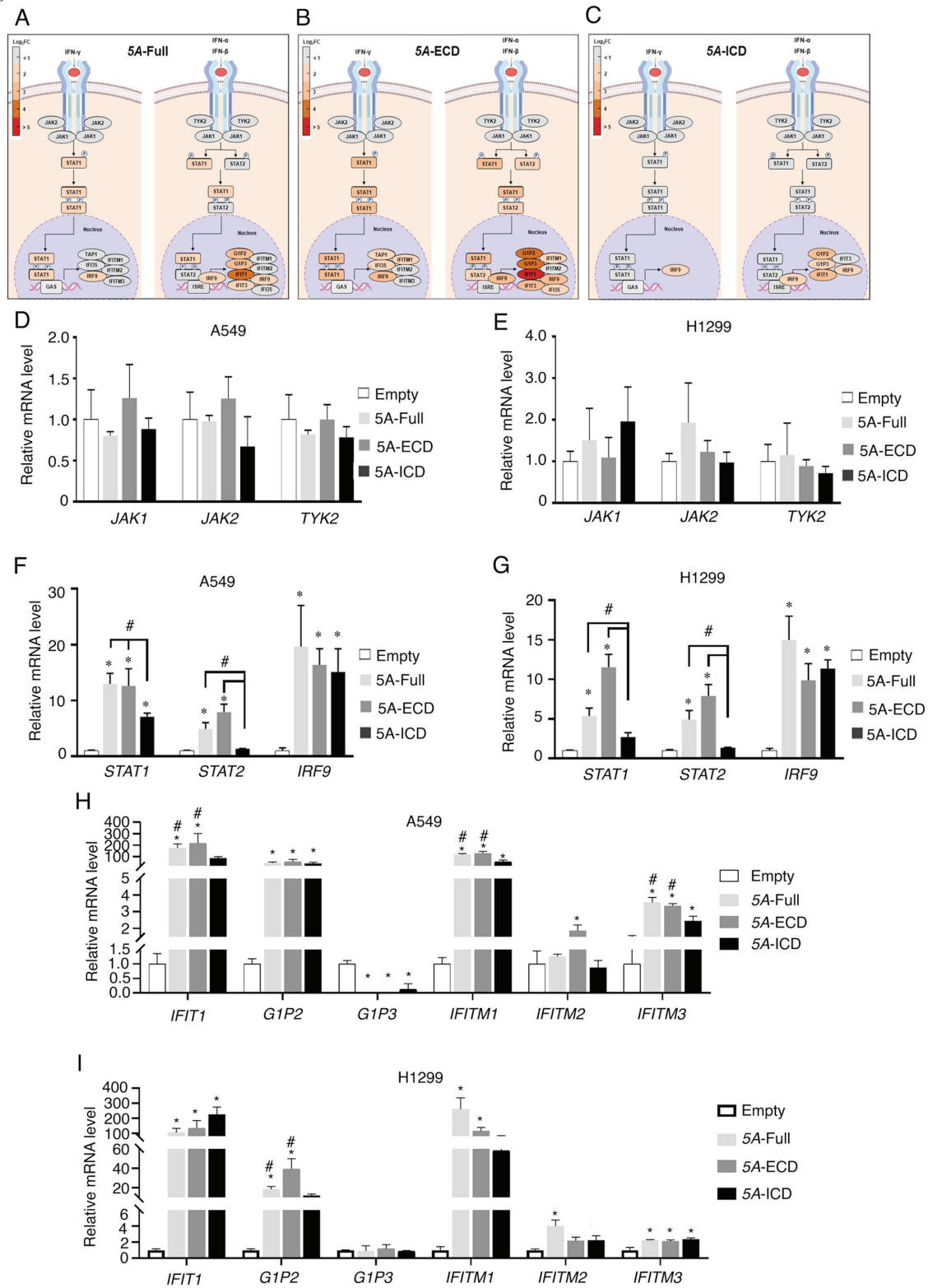


Figure 4. Expression levels of tumor suppressor genes in the interferon signaling pathway are upregulated by different SEMA5A domains. (A) Schematic depiction of the canonical pathway of interferon signaling, colored according to gene expression in the presence of 5A-Full. The darkness of red color indicates the fold change of each gene. (B) Schematic depiction of the canonical pathway of interferon signaling, colored according to gene expression in the presence of 5A-ECD. (C) Schematic depiction of the canonical pathway of interferon signaling, colored according to gene expression in the presence of 5A-ICD. (D) Relative expression levels of *JAK1*, *JAK2* and *TYK2* examined by RT-qPCR in A549 cells overexpressing different SEMA5A domains. (E) Relative expression levels of *JAK1*, *JAK2* and *TYK2* examined by RT-qPCR in H1299 cells overexpressing different SEMA5A domains. (F) Relative expression levels of *STAT1*, *STAT2* and *IRF9* in A549 cells overexpressing different SEMA5A domains. (G) Relative expression levels of *STAT1*, *STAT2* and *IRF9* in H1299 cells overexpressing different SEMA5A domains. (H) Relative expression levels of *IFIT1*, *GIP2*, *GIP3*, *IFITM1*, *IFITM2* and *IFITM3* in A549 cells overexpressing different SEMA5A domains. (I) Relative expression levels of *IFIT1*, *GIP2*, *GIP3*, *IFITM1*, *IFITM2* and *IFITM3* in H1299 cells overexpressing different SEMA5A domains. *GAPDH*: internal control. Experiments were repeated in triplicate, and the results are presented as the mean \pm SD. One-way ANOVA and Bonferroni post hoc test were performed. * $P < 0.05$ vs. empty control. # $P < 0.05$ vs. 5A-ICD. 5A-ECD, SEMA5A extracellular domain; 5A-Full, SEMA5A full length; 5A-ICD, SEMA5A intracellular domain; GIP, glycogenin 1 pseudo-gene; IFIT1, interferon induced protein with tetratricopeptide repeats 1; IFITM, interferon induced transmembrane protein; IRF9, interferon regulatory factor 9; JAK, Janus kinase; Log₂FC, log₂ fold change; RT-qPCR, reverse transcription-quantitative PCR; SEMA5A, semaphorin 5A; TYK2, tyrosine kinase 2.

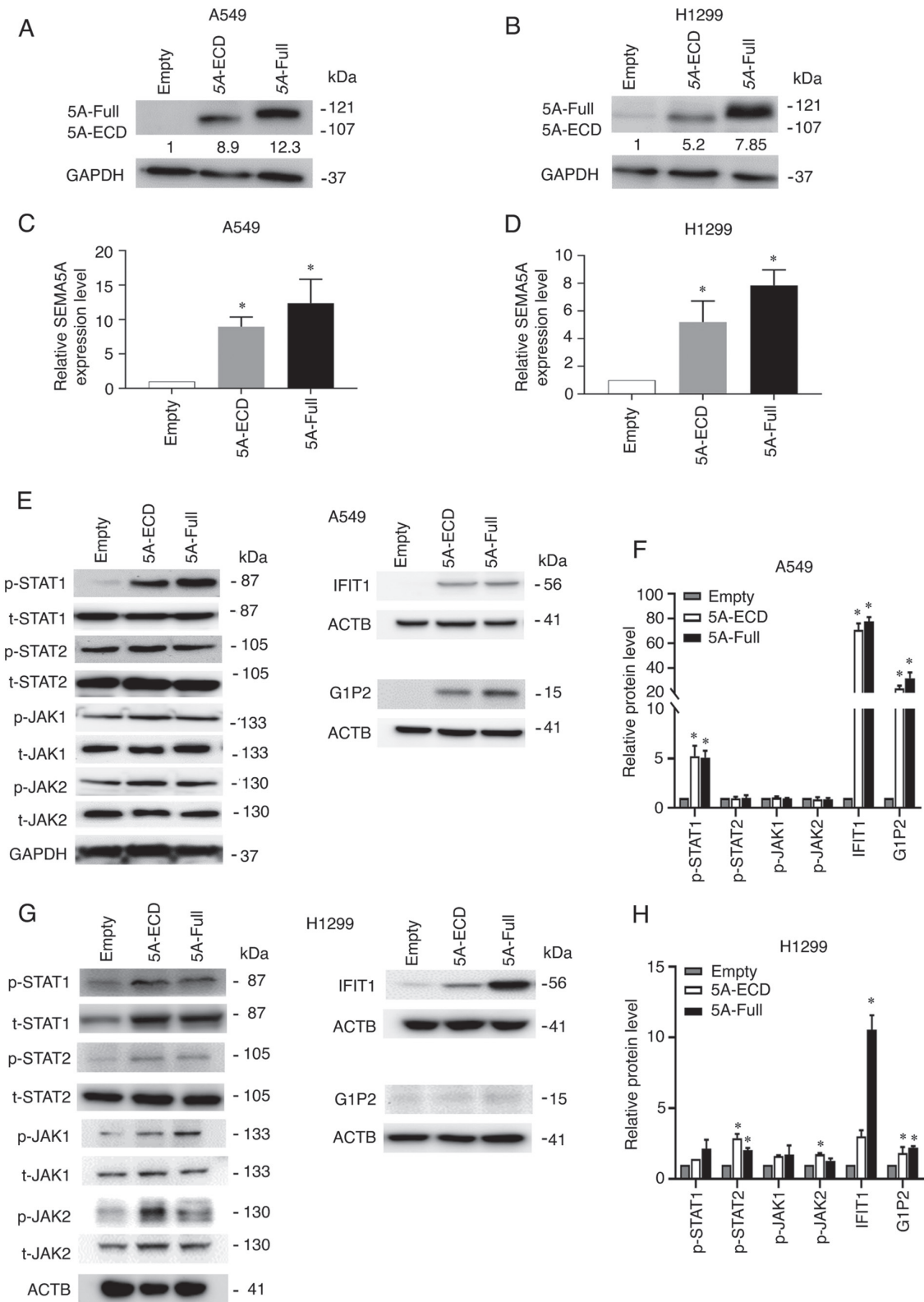


Figure 5. Overexpression of 5A-Full and 5A-ECD increases the amount of phosphorylated STAT1 in A549 cells. (A) Western blotting of total lysates from A549 cells overexpressing 5A-Full. (B) Western blotting of total lysates from H1299 cells overexpressing 5A-Full or 5A-ECD. (C) Semi-quantification of SEMA5A from the conditions of (A). (D) Semi-quantification of SEMA5A from the conditions of (B). (E) Relative protein expression levels of differentially expressed genes examined by western blotting in A549 cells. GAPDH or ACTB was used as the loading control. (F) Semi-quantification of p-STAT1, p-STAT2, p-JAK1, p-JAK2, IFIT1 and G1P2 in A549 cells. Each phosphorylated protein was normalized to its respective total protein, i.e., p-STAT1 was normalized to t-STAT1, p-STAT2 to t-STAT2, p-JAK1 to t-JAK1 and p-JAK2 to t-JAK2. IFIT1 and G1P2 were normalized to ACTB. (G) Relative protein expression levels of differentially expressed genes examined by western blotting in H1299 cells. ACTB was used as the loading control. (H) Semi-quantification of p-STAT1, IFIT1 and G1P2 in H1299 cells. Each phosphorylated protein was normalized to its respective total protein, i.e., p-STAT1 was normalized to t-STAT1, p-STAT2 to t-STAT2, p-JAK1 to t-JAK1 and p-JAK2 to t-JAK2. IFIT1 and G1P2 were normalized to ACTB. Experiments were repeated in triplicate, and the results are presented as the mean \pm SD. One-way ANOVA and Bonferroni post hoc test were performed. * P <0.05 vs. Empty. 5A-ECD, SEMA5A extracellular domain; 5A-Full, SEMA5A full length; ACTB, actin β ; G1P2, glycogenin 1 pseudogene 2; IFIT1, interferon induced protein with tetratricopeptide repeats 1; JAK, Janus kinase; p, phosphorylated; SEMA5A, semaphorin 5A; t, total.

... and 5A-ECD compared with cells overexpressing 5A-ICD (Fig. 4I). In addition, the expression levels of the identified oncogene *GIP3* were significantly decreased in A549 cells overexpressing the different SEMA5A domains, especially in the 5A-Full and 5A-ECD groups (Fig. 4H). However, no significant differences were observed in H1299 cells (Fig. 4I). Other genes, including interferon induced transmembrane protein (*IFITM1*) and *IFITM3*, were significantly upregulated (Fig. 4H and I) in both A549 and H1299 cells.

The pattern of differential gene expression in the presence of different SEMA5A domains indicated that the expression levels of differentially expressed genes in the presence of 5A-Full were similar to those in the presence of 5A-ECD, and the expression levels of *STAT1* and *STAT2* in the presence of 5A-ICD were significantly lower compared with those in the 5A-Full and 5A-ECD groups. These results suggested that overexpressing 5A-ECD may have similar effects to overexpressing 5A-Full in terms of a tumor-suppressing role in lung adenocarcinoma.

Furthermore, the protein expression levels of the DEGs were examined by western blotting. The overexpression of 5A-Full and 5A-ECD was validated by western blotting (Fig. 5A and B) and the SEMA5A protein expression was significantly increased compared with the empty control group (Fig. 5C and D). The total and phosphorylated protein expression levels of JAK1, JAK2, *STAT1* and *STAT2* were examined in A549 cells (Fig. 5E) and H1299 cells (Fig. 5G). Additionally, *IFIT1* and *GIP2*, *STAT1/2* downstream targets, were examined in A549 cells (Fig. 5E) and H1299 cells (Fig. 5G). Cells overexpressing 5A-Full and 5A-ECD exhibited significantly increased ratios of phosphorylated *STAT1* to total *STAT1* in A549 cells, and an increased ratio of phosphorylated *STAT2* to total *STAT2* in H1299 cells. Additionally, the expression levels of its downstream targets *IFIT1* and *GIP2* increased in both A549 and H1299 cells compared with empty control cells (Fig. 5E-H), which indicated that the tumor-suppressive effect of 5A-Full or 5A-ECD was due to activation of *STAT1* in the interferon signaling pathway.

Discussion

The present investigation of the tumor-suppressive mechanism of SEMA5A in lung adenocarcinoma cells revealed that overexpression of the full-length protein or the extracellular domain inhibited the proliferation and migration of both A549 and H1299 cells. Genes subject to the regulation of different SEMA5A domains were identified by microarray analysis. Among the DEGs, the most significant function of these genes was the 'Interferon Signaling' pathway. RT-qPCR demonstrated that the expression levels of several genes in this pathway, including *STAT1*, *STAT2*, *IRF9*, *IFIT1*, *GIP2* and *IFITM1*, were increased in cells expressing 5A-Full and 5A-ECD compared with the empty control group. These upregulated suppressors decreased tumor malignancy as demonstrated by the results of functional assays. Overexpression of 5A-Full or 5A-ECD inhibited the proliferation and migration of lung adenocarcinoma cells via the interferon signaling pathway.

In previous studies, SEMA5A has been identified as a tumor suppressor in lung adenocarcinoma (13,14). The present study investigated the functional role of different domains of

SEMA5A. The extracellular domain has been reported to be involved in angiogenesis (41). The expression of the extracellular domain increases both proliferation and anti-apoptosis abilities in endothelial cells (30). Furthermore, pancreatic cells transfected with the extracellular domain of SEMA5A exhibit higher metastatic potential (42). These results implied that the extracellular domain of SEMA5A has the potential to initiate carcinogenesis. However, our previous studies revealed that *SEMA5A* expression was decreased in lung cancer cells, suggesting a tumor-suppressive role (13,14). While most cancer genes are characterized as either oncogenes or tumor suppressors, some genes, such as *BRCA1*, enhancer of zeste 2 polycomb repressive complex 2 subunit, *NOTCH1*, *NOTCH2*, *STAT3* and *TP53*, have been demonstrated to display dual oncogenic and tumor suppressive functions (43,44). Therefore, it was hypothesized that *SEMA5A* has a dual oncogenic and tumor suppressor role in different types of cancer.

To further investigate the mechanism of the suppressive effects of SEMA5A in lung cancer cells, cellular functional assays were performed in A549 and H1299 cells overexpressing different SEMA5A domains. The results demonstrated that overexpressing 5A-ECD had the same effects as overexpressing 5A-Full. These two overexpression groups could inhibit the cell proliferation, colony formation and migration but had no effect on apoptosis and cell cycle progression. These results may indicate that the tumor-suppressive effects of SEMA5A are restricted to cell proliferation, and it does not have a marked effect on cell death or the cell cycle. By contrast, overexpression of 5A-ICD did not have the same tumor-suppressing effects. This demonstrated that the extracellular domain, not the intracellular domain, of SEMA5A serves the major role in inhibiting the malignancy of lung adenocarcinoma.

The present study subsequently explored the downstream genes regulated by different domains of SEMA5A by microarray analysis. The DEGs in cells expressing 5A-Full were almost identical to those in cells expressing 5A-ECD. Most of them were involved in the 'Interferon Signaling' pathway. Of the 19 DEGs common to cells overexpressing the different SEMA5A domains, 5 of them, including *STAT1*, *STAT2*, *IRF9*, *GIP2* (*ISG15*) and *IFIT1*, were in the interferon signaling pathway. Such The results of the DEGs of 5A-Full were almost identical to those of 5A-ECD, which was in line with our expectations; because ECD accounted for almost 90% of the total length, the DEGs were similar. However, the DEGs between the 5A-Full group and the 5A-ICD group were less similar. The discrepancy may be due to constructs of different domains changing the protein structure, which may lead to activation of different genes. Additionally, interplay of different domains of SEMA may change the affected genes. For example, our previous study revealed that the extracellular SEMA domain could attenuate intracellular apoptotic signaling of SEMA6A in lung cancer cells (26).

The interferon signaling pathway has been reported to have anti-proliferative, anti-angiogenic, pro-apoptotic and immunoregulatory effects in non-small cell lung cancer (37). The increase of IFN- α/β could induce *STAT1/STAT2* heterodimerization with *IRF9*, leading to the suppression of tumor growth (45). *STAT1* has been reported to improve therapeutic effects of interferons on lung cancer cells (32). *STAT2* has been demonstrated to share the anti-viral, immunomodulatory,

anti-apoptotic and anti-proliferative effects of IFN-I (36). IRF9 has been identified to decrease cell proliferation and inhibit tumor formation (35). In the present study, the expression levels of *STAT1*, *STAT2* and *IRF9* were increased in cells overexpressing 5A-Full or 5A-ECD in both A549 and H1299 cells, as were the levels of phosphorylated STAT1 in A549 cells, which revealed a tumor-suppressing mechanism in lung cancer cells.

Furthermore, *IFIT1* has been reported to be a predictive biomarker, and to suppress proliferation and promote apoptosis in cancer cells (39), and *GIP2* (*ISG15*) has been identified to promote ubiquitin E3 ligase activity and inhibit lung cancer cell proliferation in response to type I interferon (38). The present results demonstrated that the mRNA and protein expression levels *IFIT1* and *GIP2* were increased in cells overexpressing 5A-Full and 5A-ECD. Overall, these results demonstrated that the extracellular domain of SEMA5A serves a similar tumor-suppressive role as full length SEMA5A in regulating the interferon signaling pathway in lung adenocarcinoma. These results may contribute to the development of a more specific therapeutic regime to treat lung adenocarcinoma.

Acknowledgements

The authors would like to thank Dr Melissa Stauffer for editorial assistance. The authors also benefited from the technical assistance of Dr Li-Ting Jang (Biomedical Resource Core at the 1st Core Facility Lab, NTU College of Medicine, Taipei, Taiwan).

Funding

The present study was supported by grants from the Ministry of Science and Technology (grant no. MOST 109-2320-B-002-016-MY3) and National Taiwan University Hospital (grant no. MS441). The funding source had no role in the design of this study and will not have any role in its execution or analysis, interpretation of the data, or the decision to publish the results.

Availability of data and materials

The microarray datasets generated during the current study are available in the Gene Expression Omnibus repository (<https://www.ncbi.nlm.nih.gov/geo/query/acc.cgi?acc=GSE157062>). All other data generated or analyzed during this study are included in this published article.

Authors' contributions

MZC, HHH and LCL conceived and designed the experiments. MZC, LYS and MHH performed the experiments. MZC, PHK, LLC and TPL analyzed the data. LHC, EYC, LPC and MHT contributed reagents, materials and/or analysis tools, interpreted data and revised the manuscript critically for important intellectual content. MZC, LYS, MHH and LCL confirmed the authenticity of all the raw data. MZC and LCL wrote the paper. All authors have read and approved the final manuscript, and agreed to be accountable for all aspects of the work in ensuring that questions related to the accuracy or

integrity of any part of the work are appropriately investigated and resolved.

Ethics approval and consent to participate

The gene recombinant/infectious biological materials experiments were approved by the Biosafety Committee of the College of Medicine, National Taiwan University (BG1050086; Taipei, Taiwan).

Patient consent for publication

Not applicable.

Competing interests

The authors declare that they have no competing interests.

References

1. Bray F, Ferlay J, Soerjomataram I, Siegel RL, Torre LA and Jemal A: Global cancer statistics 2018: GLOBOCAN estimates of incidence and mortality worldwide for 36 cancers in 185 countries. *CA Cancer J Clin* 68: 394-424, 2018.
2. Torre LA, Siegel RL and Jemal A: Lung cancer statistics. In: Lung cancer and personalized medicine. Springer, New York, NY, pp1-19, 2016.
3. Molina JR, Yang P, Cassivi SD, Schild SE and Adjei AA: Non-small cell lung cancer: Epidemiology, risk factors, treatment, and survivorship. *Mayo Clin Proc* 83: 584-594, 2008.
4. Ettinger DS, Akerley W, Bepler G, Blum MG, Chang A, Cheney RT, Chirieac LR, D'Amico TA, Demmy TL, Ganti AK, *et al*: Non-small cell lung cancer. *J Natl Compr Canc Netw* 8: 740-801, 2010.
5. Chang JS, Chen LT, Shan YS, Lin SF, Hsiao SY, Tsai CR, Yu SJ and Tsai HJ: Comprehensive analysis of the incidence and survival patterns of lung cancer by histologies, including rare subtypes, in the era of molecular medicine and targeted therapy: A nation-wide cancer registry-based study from Taiwan. *Medicine (Baltimore)* 94: e969, 2015.
6. Ger LP, Liou SH, Shen CY, Kao SJ and Chen KT: Risk factors of lung cancer. *J Formos Med Assoc* 91 (Suppl 3): S222-S231, 1992 (In Japanese).
7. Hirayasu T, Iwamasa T, Kamada Y, Koyanagi Y, Usuda H and Genka K: Human papillomavirus DNA in squamous cell carcinoma of the lung. *J Clin Pathol* 49: 810-817, 1996.
8. Yamamoto H, Shigematsu H, Nomura M, Lockwood WW, Sato M, Okumura N, Soh J, Suzuki M, Wistuba II, Fong KM, *et al*: PIK3CA mutations and copy number gains in human lung cancers. *Cancer Res* 68: 6913-6921, 2008.
9. Eberhard DA, Johnson BE, Amler LC, Goddard AD, Heldens SL, Herbst RS, Ince WL, Jänne PA, Januario T, Johnson DH, *et al*: Mutations in the epidermal growth factor receptor and in KRAS are predictive and prognostic indicators in patients with non-small-cell lung cancer treated with chemotherapy alone and in combination with erlotinib. *J Clin Oncol* 23: 5900-5909, 2005.
10. Shigematsu H, Lin L, Takahashi T, Nomura M, Suzuki M, Wistuba II, Fong KM, Lee H, Toyooka S, Shimizu N, *et al*: Clinical and biological features associated with epidermal growth factor receptor gene mutations in lung cancers. *J Natl Cancer Inst* 97: 339-346, 2005.
11. Toyooka S, Tsuda T and Gazdar AF: The TP53 gene, tobacco exposure, and lung cancer. *Hum Mutat* 21: 229-239, 2003.
12. Hainaut P and Pfeifer GP: Patterns of p53 G->T transversions in lung cancers reflect the primary mutagenic signature of DNA-damage by tobacco smoke. *Carcinogenesis* 22: 367-374, 2001.
13. Lu TP, Tsai MH, Lee JM, Hsu CP, Chen PC, Lin CW, Shih JY, Yang PC, Hsiao CK, Lai LC and Chuang EY: Identification of a novel biomarker, SEMA5A, for non-small cell lung carcinoma in nonsmoking women. *Cancer Epidemiol Biomarkers Prev* 19: 2590-2597, 2010.

- enka G, Chen YA, Chuang EY, Tsai MH, Sher YP and Lai LC: Semaphorin 5A suppresses the proliferation and migration of lung adenocarcinoma cells. *Int J Oncol* 56: 165-177, 2020.
15. Unified nomenclature for the semaphorins/collapsins. Semaphorin Nomenclature Committee. *Cell* 97: 551-552, 1999.
 16. Gherardi E, Love CA, Esnouf RM and Jones EY: The sema domain. *Curr Opin Struct Biol* 14: 669-678, 2004.
 17. Hota PK and Buck M: Plexin structures are coming: Opportunities for multilevel investigations of semaphorin guidance receptors, their cell signaling mechanisms, and functions. *Cell Mol Life Sci* 69: 3765-3805, 2012.
 18. Pasterkamp RJ and Giger RJ: Semaphorin function in neural plasticity and disease. *Curr Opin Neurobiol* 19: 263-274, 2009.
 19. Delaire S, Elhabazi A, Bensussan A and Boumsell L: CD100 is a leukocyte semaphorin. *Cell Mol Life Sci* 54: 1265-1276, 1998.
 20. Bougeret C, Mansur IG, Dastot H, Schmid M, Mahouy G, Bensussan A and Boumsell L: Increased surface expression of a newly identified 150-kDa dimer early after human T lymphocyte activation. *J Immunol* 148: 318-323, 1992.
 21. Gitler AD, Lu MM and Epstein JA: PlexinD1 and semaphorin signaling are required in endothelial cells for cardiovascular development. *Dev Cell* 7: 107-116, 2004.
 22. Hayashi M, Nakashima T, Taniguchi M, Kodama T, Kumanogoh A and Takayanagi H: Osteoprotection by semaphorin 3A. *Nature* 485: 69-74, 2012.
 23. Roche J, Boldog F, Robinson M, Varella-Garcia M, Swanton M, Waggoner B, Fishel R, Franklin W, Gemmill R, Drabkin H, *et al*: Distinct 3p21.3 deletions in lung cancer and identification of a new human semaphorin. *Oncogene* 12: 1289-1297, 1996.
 24. Basile JR, Castilho RM, Williams VP and Gutkind JS: Semaphorin 4D provides a link between axon guidance processes and tumor-induced angiogenesis. *Proc Natl Acad Sci USA* 103: 9017-9022, 2006.
 25. Tomizawa Y, Sekido Y, Kondo M, Gao B, Yokota J, Roche J, Drabkin H, Lerman MI, Gazdar AF and Minna JD: Inhibition of lung cancer cell growth and induction of apoptosis after reexpression of 3p21.3 candidate tumor suppressor gene SEMA3B. *Proc Natl Acad Sci USA* 98: 13954-13959, 2001.
 26. Shen CY, Chang YC, Chen LH, Lin WC, Lee YH, Yeh ST, Chen HK, Fang W, Hsu CP, Lee JM, *et al*: The extracellular SEMA domain attenuates intracellular apoptotic signaling of semaphorin 6A in lung cancer cells. *Oncogenesis* 7: 95, 2018.
 27. Li X and Lee AY: Semaphorin 5A and plexin-B3 inhibit human glioma cell motility through RhoGDIalpha-mediated inactivation of Rac1 GTPase. *J Biol Chem* 285: 32436-32445, 2010.
 28. Sadanandam A, Sidhu SS, Wullschlegel S, Singh S, Varney ML, Yang CS, Ashour AE, Batra SK and Singh RK: Secreted semaphorin 5A suppressed pancreatic tumour burden but increased metastasis and endothelial cell proliferation. *Br J Cancer* 107: 501-507, 2012.
 29. Saxena S, Purohit A, Varney ML, Hayashi Y and Singh RK: Semaphorin-5A maintains epithelial phenotype of malignant pancreatic cancer cells. *BMC Cancer* 18: 1283, 2018.
 30. Livak KJ and Schmittgen TD: Analysis of relative gene expression data using real-time quantitative PCR and the 2(-Delta Delta C(T)) method. *Methods* 25: 402-408, 2001.
 31. Sturn A, Quackenbush J and Trajanoski Z: Genesis: Cluster analysis of microarray data. *Bioinformatics* 18: 207-208, 2002.
 32. Chen J, Zhao J, Chen L, Dong N, Ying Z, Cai Z, Ji D, Zhang Y, Dong L, Li Y, *et al*: STAT1 modification improves therapeutic effects of interferons on lung cancer cells. *J Transl Med* 13: 293, 2015.
 33. Cheriya V, Kaur J, Davenport A, Khaleel A, Chowdhury N and Gaddipati L: G1P3 (IFI6), a mitochondrial localised antiapoptotic protein, promotes metastatic potential of breast cancer cells through mtROS. *Br J Cancer* 119: 52-64, 2018.
 34. Gao M, Lin Y, Liu X, Li Y, Zhang C, Wang Z, Wang Z, Wang Y and Guo Z: ISG20 promotes local tumor immunity and contributes to poor survival in human glioma. *Oncoimmunology* 8: e1534038, 2019.
 35. Luker KE, Pica CM, Schreiber RD and Piwnicka-Worms D: Overexpression of IRF9 confers resistance to antimicrotubule agents in breast cancer cells. *Cancer Res* 61: 6540-6547, 2001.
 36. Park C, Li S, Cha E and Schindler C: Immune response in Stat2 knockout mice. *Immunity* 13: 795-804, 2000.
 37. Wilderman MJ, Sun J, Jassar AS, Kapoor V, Khan M, Vachani A, Suzuki E, Kinniry PA, Serman DH, Kaiser LR and Albelda SM: Intrapulmonary IFN-beta gene therapy using an adenoviral vector is highly effective in a murine orthotopic model of bronchogenic adenocarcinoma of the lung. *Cancer Res* 65: 8379-8387, 2005.
 38. Yoo L, Yoon AR, Yun CO and Chung KC: Covalent ISG15 conjugation to CHIP promotes its ubiquitin E3 ligase activity and inhibits lung cancer cell growth in response to type I interferon. *Cell Death Dis* 9: 97, 2018.
 39. Zhang JF, Chen Y, Lin GS, Zhang JD, Tang WL, Huang JH, Chen JS, Wang XF and Lin ZX: High IFIT1 expression predicts improved clinical outcome, and IFIT1 along with MGMT more accurately predicts prognosis in newly diagnosed glioblastoma. *Hum Pathol* 52: 136-144, 2016.
 40. Ghislain JJ, Wong T, Nguyen M and Fish EN: The interferon-inducible stat2:Stat1 heterodimer preferentially binds in vitro to a consensus element found in the promoters of a subset of interferon-stimulated genes. *J Interferon Cytokine Res* 21: 379-388, 2001.
 41. Sadanandam A, Rosenbaugh EG, Singh S, Varney M and Singh RK: Semaphorin 5A promotes angiogenesis by increasing endothelial cell proliferation, migration, and decreasing apoptosis. *Microvasc Res* 79: 1-9, 2010.
 42. Sadanandam A, Varney ML, Singh S, Ashour AE, Moniaux N, Deb S, Lele SM, Batra SK and Singh RK: High gene expression of semaphorin 5A in pancreatic cancer is associated with tumor growth, invasion and metastasis. *Int J Cancer* 127: 1373-1383, 2010.
 43. Aranko AS, Oemig JS, Kajander T and Iwai H: Intermolecular domain swapping induces intein-mediated protein alternative splicing. *Nat Chem Biol* 9: 616-622, 2013.
 44. Shen L, Shi Q and Wang W: Double agents: Genes with both oncogenic and tumor-suppressor functions. *Oncogenesis* 7: 25, 2018.
 45. Fink K and Grandvaux N: STAT2 and IRF9: Beyond ISGF3. *JAKSTAT* 2: e27521, 2013.